Molecular Ordering and the Direct Measurement of Weak Proton−Proton Dipolar Interactions in a Rubber Network

P. T. Callaghan*,† and E. T. Samulski‡

Department of Physics, Massey University, Palmerston North, New Zealand, and Department of Chemistry, University of North Carolina, Chapel Hill, North Carolina 27599

Received May 30, 1996; Revised Manuscript Received August 23, 1996[⊗]

ABSTRACT: We demonstrate a new NMR technique that is suitable for the measurement of weak proton dipolar interactions in fluid polymers where rapid segmental dynamics "preaverage" the rigid-lattice dipolar coupling. The method is especially applicable to polymer melts and networks, where such residual interactions can provide valuable insight regarding molecular order and reorientational dynamics. We use this method to study natural rubber under uniaxial stretching. By measuring the residual dipolar coupling and its orientation dependence, we are able to distinguish the influence of chain stretching from chain reorientation in the deformation process. The pulse sequence we employ directly generates a function β, which is zero in the absence of dipolar interactions, which is completely independent of all Zeeman dephasing associated with chemical shifts or magnetic inhomogeneity, and whose time dependence can yield both the magnitude and the fluctuation rate of the residual dipolar interaction.

Introduction

Nuclear magnetic resonance has been a profoundly useful technique for providing insights into segmental dynamics in dilute polymer solutions through measurements of spin relaxation times. Recent advances in solid state NMR give access to a wide range of dynamical processes in solid polymers. While the dipole−dipole interaction between a pair of protons is inherently the most sensitive way to elicit dynamical information from NMR, it has severe limitations in the condensed fluid phases of polymers, where magnetic interactions preclude their measurement. We have developed a method to circumvent this problem and demonstrate this with a natural rubber network, wherein we can systematically alter the magnitude of the residual dipolar interactions by mechanically deforming the sample. The methodology we propose is generally applicable to partially averaged proton dipolar interactions and opens the way to studying segmental order and its associated dynamics in a variety of fluid polymer networks or entangled melts and solutions (transient networks) without the need for nuclear isotopic labeling.

Dynamical processes in the condensed fluid phases of entangled polymers—melts, concentrated solutions, and amorphous networks above the glass transition—occur over a wide range of time scales. These include fast, localized processes like intramonomer librations ($\sim 10^{-12}$ s time scale) and correlated conformer isomerizations ($\leq 10^{-9}$ s), which are comparable to motions in liquids comprised of flexible, low molar mass molecules. In contrast with such liquids, though, the concatenation of monomers imposes constraints on molecular motions that give rise to slow dynamical processes unique to polymer chains. For example, the so-called Rouse modes correspond to subchain reorientations that may exhibit dynamics on the microsecond time scale. And cooperative multichain processes that involve whole-chain reconfigurational dynamics (e.g., reptative diffusion) can be operative on a tens of seconds time scale for high molar mass polymers. Consequently, the way in which microscopic properties appear to be averaged will depend on the time scale of the experimental window associated with the particular technique employed.

Among the many important average molecular properties that can be measured by NMR is the local order parameter associated with nuclear spin interactions of rank 2 tensorial character. In particular, these include the proton−proton dipolar interaction of magnitude $\nu_H = (3/2)\gamma^2\hbar r^{-3}$, associated with a pair of protons affixed at a separation r within a monomer, and the quadrupolar interation of magnitude $\nu_D = (3/4)e^2Qq/\hbar$ experienced by deuterons in the presence of a magnetic field gradient q associated with the local molecular orbital. These interactions, which are bilinear in the spin operators, transform under rotation as $P_2(\cos\vartheta) = (1/2)[3\cos^2\vartheta(t) - 1]$, where $\vartheta(t)$ is the angle the polarizing magnetic field makes with the internuclear vector in the case of the pair of protons, or the electric field gradient symmetry axis in the case of deuterons. The corresponding local order parameters involve the temporal average over relevant dynamical processes. In the case of isotropic polymer melts or solutions, $\overline{P_2(\cos\vartheta)} = 0$ on a sufficiently long time scale. However, on the operative NMR time scale, $[\nu_{H,D}]^{-1} \approx 10^{-6}$ s, the whole-chain reconfigurational processes are too slow, and the rank 2 spin interactions are incompletely averaged. J.-P. Cohen Addad originally suggested that one might investigate aspects of the topological restrictions in networks and entangled phases ("slow" dynamical processes) by studying *residual* nuclear spin interactions—dipolar and quadrupolar interactions that have been preaveraged over the "fast" dynamical processes.[1,2] Subsequently, it was shown that, in mechanically ordered fluid polymers—deformed networks and sheared melts—$\overline{P_2(\cos\vartheta)} \neq 0$, irrespective of the time scale. In particular, the deuterium NMR spectroscopic signature of mechanically induced anisotropy, the quadrupolar splitting ($2\nu_D\overline{P_2(\cos\vartheta)}$), has been extensively studied.[3−6]

In principle, knowledge about the strength of the dipolar and quadrupolar interactions and the orientation distribution of their relevant principal axes can reveal important information about local order and dynamics. In practice, such knowledge depends on the effectiveness with which the interaction can be distin-

† Massey University.
‡ University of North Carolina.
⊗ Abstract published in *Advance ACS Abstracts,* December 1, 1996.

S0024-9297(96)00784-X CCC: $14.00

guished from other terms in the nuclear spin Hamiltonian, especially from those associated with Zeeman-like magnetic interactions. In the case of ^{2}H-NMR, this distinguishability is relatively straightforward and has led to the widespread use of deuterium labeling experiments. However, in many applications, the chemical modification required to uniquely label with a deuteron probe is impractical. Even where labeling is possible, the much lower sensitivity of ^{2}H-NMR makes the use of this method prohibitively time consuming in a wide class of experiments. By contrast, the use of proton NMR to gain information about molecular order has a number of attractive features. However, the method traditionally suffers from the often overwhelming dominance of the remaining (non-dipolar) magnetic interactions.

The existence of residual interactions for protons will be especially important for polymers above their glass transition or melting temperatures, wherein topological restrictions hinder isotropic reorientation of chain segments. In polymer networks, the covalent cross-links (and entanglements) prevent isotropic reconfigurations of the chains, while in melts, complete motional averaging is inhibited by the persistence of entanglements on the NMR time scale. The relevant time scale is, in fact, $[\Delta]^{-1} \approx 10^{-3}-10^{-4}$ s, corresponding to a transient, residual dipolar interaction, $\Delta = \nu_H P_2(\cos \vartheta)$. The magnitude of Δ often corresponds to a reduction of the static dipolar interaction, ν_H, by 2 or more orders of magnitude by preaveraging $P_2(\cos \vartheta)$ over the stochastically independent and nearly isotropic "fast" motion of the chain segments. The size of the residual dipolar interaction may then be comparable to the spread in Zeeman energies associated with the chemical shift. Moreover, the comparatively delicate nature of the residual proton dipolar interaction in such materials may be exacerbated by sample geometries highly unfavorable to magnetic field homogeneity. Therefore, in addition to chemical shift effects, the spectrum of proton precession frequencies may be dominated by inhomogeneous broadening of Zeeman origin. Such circumstances may arise in experiments where the sample has undesirable surface symmetry (nonspherical network fragments), where it has diamagnetic filler particles, or where it is contained in a diamagnetic goniometer, jig, or shear cell.

Here we report on a means of extracting information about both the magnitude and dynamics of small residual proton dipolar interactions and demonstrate the application of this method to observe the degree of order induced in natural rubber upon stretching. The method is shown to be effective even in the presence of strong and undesirable magnetic interactions.

Theory of Spin Echoes and Dipolar Interactions. In a series of papers published in the early 1970s,[7] J.-P. Cohen Addad suggested that weak, rank 2 tensorial interactions present in entangled polymers might be observed in a convenient manner by means of a combination of "solid echo" pulses trains and the free induction decay following a simple 90° pulse. By appropriately superposing the signals obtained under three different pulse sequences, it is possible to derive a function, Γ, which is directly sensitive to correlations in the precessional motion of the spins under the tensorial interaction. The dynamical nature of the weak interactions isolated by this method was later demonstrated by Collignon *et al.*[8] in the case of proton dipolar and deuterium quadrupole interactions for polyethylene melts in a highly *homogeneous* magnetic field.

The method of Cohen Addad, while effective in the case of deuterons, is difficult to implement for proton dipolar interactions. In particular, the method suffers from the persistent influence of magnetic dephasing due to a coefficient in Γ arising directly from the Zeeman interactions. This can result in a domination of the Γ function's time dependence by unwanted terms in the spin Hamiltonian, especially where proton chemical shift effects or local field inhomogeneity effects are significant. Our alternative strategy is to implement a pulse sequence that is capable of generating the desired correlation function directly and in a manner that completely refocuses all magnetic precession.

In the argument presented here, we follow the notation introduced by Collignon *et al.* We allow for a spin Hamiltonian in which a given spin experiences, in addition to the dominant Larmor precession in the polarizing magnetic field, two additional (or offset) interactions. The first, which is linear in the spin operator with associated precession frequency δ, comprises all additional Zeeman interactions such as those associated with chemical shift or local field homogeneity. The second, which is bilinear in the spin operators with associated precession frequency Δ, will arise from the dipolar interaction between proton spin pairs. Because of the dependence of this latter frequency on the orientation of the internuclear vector, we allow that it is time-dependant in accordance with the motion of the molecular segment in which the spin pair resides. Following a 90° radio frequency (rf) pulse, we may describe the ensemble-averaged, in-phase magnetization for such isochromats of the spin system as

$$S_0(t) = \langle \cos \delta t \cos \phi(0,t) \rangle \tag{1}$$

where t is the evolution time following the rf pulse, and the dipolar phase angle, ϕ, is given by

$$\phi(t_1,t_2) = \int_{t_1}^{t_2} \Delta(t')\, dt' \tag{2}$$

For convenience, we may write the separate ensemble average over the Zeeman precession as

$$G(t) = \langle \cos \delta t \rangle_\delta \tag{3}$$

Next we consider the effect of these precessions in the case of four separate experiments in which we apply combinations of rf pulses, Θ_{α_n}, where Θ is the nutation angle and the subscript α_n denotes the relative phase of the nth pulse. The experiments comprise the free induction decay pulse sequence consisting only of a single $90°_x$ pulse; the "solid echo" sequences, $90°_x-\tau-90°_{x,y}$; and the "Hahn echo", $90°_x-\tau-180°_y$, where, in the echo examples, τ is the time separating the rf pulses. In each case, we allow that the density matrix that describes the nuclear spin ensemble will evolve under the influence of the two offset terms in the Hamiltonian. The details of these evolutions are well known and can be found in standard texts.[9] The results are as follows:

free induction decay

$$S_0(t) = G(t)\langle \cos \phi(0,t) \rangle \tag{4}$$

solid echo, $90°_x-\tau-90°_y$

$$S_1(t,\tau) = {}^1/_2[G(t) + G(2\tau - t)]\langle \cos[\phi(0,\tau) - \phi(\tau,t)] \rangle \tag{5}$$

solid echo, $90°_x-\tau-90°_x$

$$S_2(t,\tau) = {}^1/_2[G(t) - G(2\tau - t)]\langle\cos[\phi(0,\tau) - \phi(\tau,t)]\rangle \quad (6)$$

Hahn echo, $90°_x-\tau-180°_y$

$$S_3(t,\tau) = G(2\tau - t)\langle\cos[\phi(0,\tau) + \phi(\tau,t)]\rangle \quad (7)$$

where, in each case, t represents the time delay before sampling as measured from the initial $90°_x$ pulse. In the Cohen Addad scheme, one computes the function $\Gamma(t,\tau)$, where

$$\Gamma(t,\tau) = [S_1(t,\tau) + S_2(t,\tau) - S_0(t)]/2S_0(0)$$

$$= G(t)\langle\sin\phi(0,\tau)\sin\phi(\tau,t)\rangle \quad (8)$$

Note that Γ comprises two factors, one arising from the Zeeman precession and the other a sine correlation function due to the dipolar precession. Despite the factorization of these terms into separate ensemble averages, the interesting time dependence of the dipolar correlation may be masked by a dominant Zeeman precession $G(t)$. We propose, instead, a different combination involving the solid echoes and the Hahn echo. The scheme is similar to a qualitative experiment proposed by one of us in an earlier paper.[10] The new superposition, which we term $\beta(t,\tau)$, is given by

$$\beta(t,\tau) = [S_1(t,\tau) - S_2(t,\tau) - S_3(t,\tau)]/2S_3(0,0)$$

$$= G(2\tau - t)\langle\sin\phi(0,\tau)\sin\phi(\tau,t)\rangle \quad (9)$$

The time $t = 2\tau$ corresponds to the instant when the magnetic precessions are refocused in the spin echo. At that particular instant, the effect of Zeeman precession vanishes ($G(0) = 1$), leaving the result

$$\beta(2\tau,\tau) = \langle\sin\phi(0,\tau)\sin\phi(\tau,2\tau)\rangle \quad (10)$$

This one-dimensional function is ideally suited to revealing the weak dipolar interactions and their fluctuations without perturbations due to Zeeman effects.

The dipolar correlation function, $\langle\sin\phi(0,\tau)\sin\phi(\tau,t)\rangle$, has a number of interesting properties. It is a null function in the absence of dipolar interactions. This means that the appearance of a non-zero result for β is indicative of terms in the Hamiltonian bilinear in the spin operators. Furthermore, the function is zero in the limit that t (and τ) approaches zero. This limiting short time behavior of the correlation $\langle\sin\phi(0,\tau)\sin\phi(\tau,t)\rangle$ is both interesting and useful. For example, Collignon *et al.* have pointed out[2] that, where both $\phi(0,\tau)$ and $\phi(\tau,t) \ll \pi/2$ (the small phase angle limit), one may write

$$\langle\sin\phi(0,\tau)\sin\phi(\tau,t)\rangle \approx \langle\phi(0,\tau)\phi(\tau,t)\rangle$$

$$= \int_0^t dt' \int_\tau^t dt'' \langle\Delta(t')\Delta(t'')\rangle \quad (11)$$

The simplest possible description of the phase angle correlation, $\langle\Delta(t')\Delta(t'')\rangle$, is given by the stationary Markoff function, $\langle\Delta^2\rangle\exp(-|t'-t''|/2\tau_\Delta)$, where $\tau_\Delta$is the correlation time for the fluctuating dipolar interaction. Using this function, one finds

$$\beta(2\tau,\tau) = \langle\Delta^2\rangle\tau_\Delta{}^2[1 + \exp(-2\tau/\tau_\Delta) - 2\exp(-\tau/\tau_\Delta)]$$

$$\approx \langle\Delta^2\rangle\tau^2\exp(-\tau/\tau_\Delta) \quad (12)$$

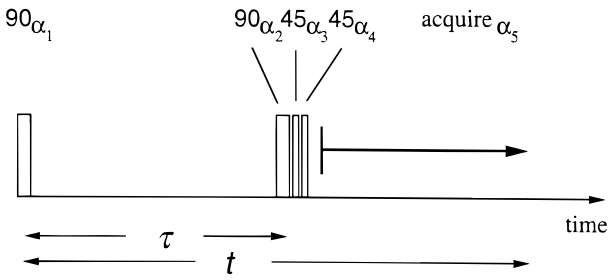

Figure 1. Radiofrequency pulse sequence used to acquire the $\beta(t,\tau)$ and $\Gamma(t,\tau)$ functions directly. The associated phase cycles are given in Table 1.

It should be stressed that this equation assumes a simple exponential correlation function and will be valid only when $\tau \lesssim \langle\Delta^2\rangle^{1/2}$. Furthermore, it takes no account of other processes which result in a decay of transverse magnetization. These include relaxation effects arising from the rapid (preaveraging) fluctuations of the dipolar interactions as well as stochastic effects arising from purely Zeeman origin. Such additional relaxation may be incorporated by including in eq 12 an empirical factor, $\exp\{-2\tau/T_2\}$, where T_2 may be independently determined. A more exact evaluation of eq 11 appropriate to general correlation functions and valid over all time scales is available and will be the subject of a separate publication.[11] However, for the purposes of the present study, eq 12 will serve us well within the limits of vailidity specified.

Experimental Implementation

An efficient pulse sequence that implements the $\beta(t,\tau)$ function directly is shown in Figure 1. The composite of one 90_{α_n} and two 45_{α_m} pulses can be used to simulate a null pulse, a single 90° pulse, or a single 180° pulse, depending on the phases α_n and α_m. The phase cycle appropriate to this sequence is shown in Table 1. It incorporates an eight-step cyclops sequence along with the phase triplet required to implement the basic $\beta(t,\tau)$ superposition. While it is possible to generate this superposition by subsequently combining the results from three separate experiments corresponding to the three separate pulse sequences, the direct implementation has the advantage that it is less susceptible to errors due to variation in magnetic field or spectrometer gain.

We have implemented the $\beta(t,\tau)$ pulse sequence on a Bruker AMX300 NMR spectrometer, along with a similar sequence (but with different phase cycle; Table 1), which results in the $\Gamma(t,\tau)$ function of Cohen Addad. A comparison between the effectiveness of these two sequences in shown in Figure 2, where we plot signal intensity contours of $\beta(t,\tau)$ and $\Gamma(t,\tau)$, respectively, for the proton NMR signal obtained from a natural rubber network—cross-linked *cis*-1,4-polyisoprene filled with treated clay. The $\Gamma(t,\tau)$ function clearly suffers severely from the decays due to T_2* relaxation, so much so that the rising dipolar sine correlation function is completely overwhelmed. In Figure 3, we compare $\beta(t,\tau)$ (●) and $\Gamma(t,\tau)$ (○) at the time $t = 2\tau$, where the significant reduction in signal for the latter function is apparent. (In more homogeneous samples, oscillations and dephasing due to a distribution of chemical shifts is also apparent in $\Gamma(2\tau,\tau)$.) By contrast, at the time $t = 2\tau$, the $\beta(t,\tau)$ exhibits an echo maximum at which all Zeeman dephasing is removed.

Dipolar Interactions in Stretched Natural Rubber

We now describe experiments in which the β function is used to determine the degree of residual dipolar order in the cross-linked polyisoprene chains of natural rubber. The principal objective of this study will be to investigate the degree of chain alignment produced under uniaxial extension of the network.

Table 1. Phase Cycles for Implementing $\beta(t,\tau)$ and $\Gamma(t,\tau)$ Using the Four-Pulse Sequence in Figure 1[a]

	β cycle																							
phase[b]	1	2	3	4	5	6	7	8	9	10	11	12	13	14	15	16	17	18	19	20	21	22	23	24
α_1	0	0	0	0	0	0	2	2	2	2	2	2	1	1	1	1	1	1	3	3	3	3	3	3
α_2	1	0	1	3	2	3	1	0	1	3	2	3	2	1	2	0	3	0	2	1	2	0	3	0
α_3	1	1	1	3	3	3	1	1	1	3	3	3	2	2	2	0	0	0	2	2	2	0	0	0
α_4	3	3	1	1	1	3	3	3	1	1	1	3	0	0	2	2	2	0	0	0	2	2	2	0
$\alpha_{acquire}$	0	2	2	0	2	2	2	0	0	2	0	0	1	3	3	1	3	3	3	1	1	3	1	1
sequence: $S_1 - S_2 - S_3$ ...																								
	Γ cycle																							
phase[b]	1	2	3	4	5	6	7	8	9	10	11	12	13	14	15	16	17	18	19	20	21	22	23	24
α_1	0	0	0	0	0	0	2	2	2	2	2	2	1	1	1	1	1	1	3	3	3	3	3	3
α_2	1	0	1	3	2	3	1	0	1	3	2	3	2	1	2	0	3	0	2	1	2	0	3	0
α_3	1	1	3	3	3	1	1	1	3	3	3	1	2	2	0	0	0	2	2	2	0	0	0	2
α_4	3	3	3	1	1	1	3	3	3	1	1	1	0	0	0	2	2	2	0	0	0	2	2	2
α_{aquire}	0	0	2	0	0	2	2	2	0	2	2	0	1	1	3	1	1	3	3	3	1	3	3	1
sequence: $S_1 + S_2 - S_0$ ...																								

[a] The total cycle consists of a convolution of the three-phase cycle segment to implement eqs 8 and 9 and an eight-step phase cycle designed to correct for spectrometer artifacts. [b] The phases 0, 1, 2, and 3 correspond to x, y, $-x$, and $-y$, respectively.

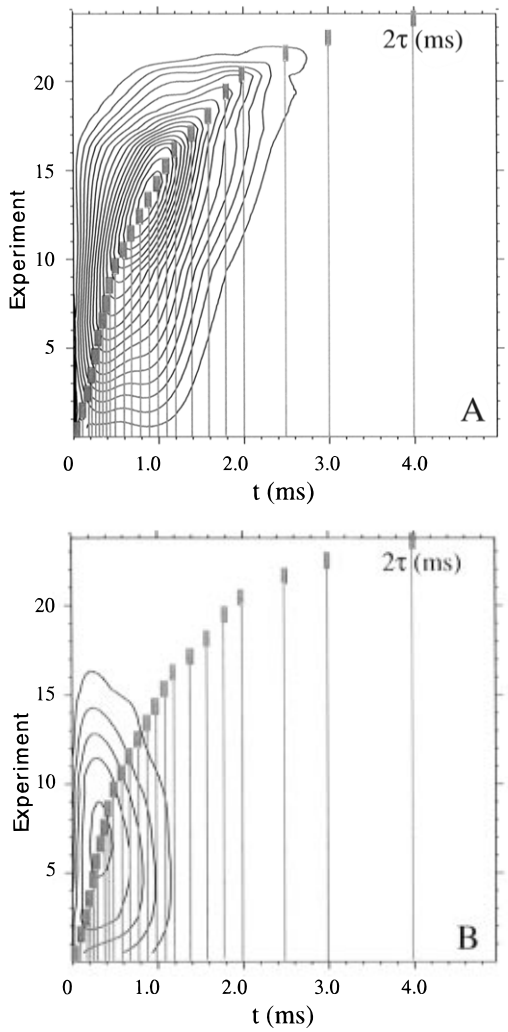

Figure 2. (A) $\beta(t,\tau)$ and (B) $\Gamma(t,\tau)$, the proton NMR signal intensity contours derived from a natural rubber sample. A series of 24 experiments is shown where the τ value is changed from 0.05 to 4.0 ms; the vertical lines indicate the 2τ value (sampling points for extracting the $\beta(2\tau,\tau)$ and $\Gamma(2\tau,\tau)$ functions).

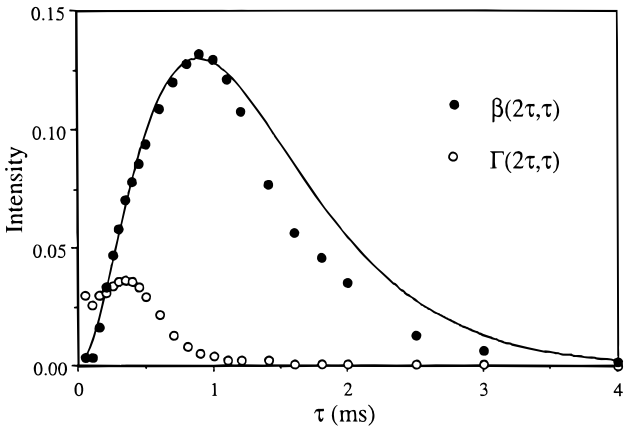

Figure 3. Comparison of $\beta(t,\tau)$ (●) and $\Gamma(t,t)$ (○) for $t = 2\tau$; the solid line is derived from eq 12 (see text).

(i) Theory of Uniaxial Extension. The averaged second moment is a measure of the residual dipolar order in the polymer chains in the natural rubber after the preaveraging process associated with rapid segmental reorientation. We shall show here, in the case where the rubber network is extended, that this parameter also gives a measure of the chain alignment.

In the equilibrium (unstretched) state of the rubber, the end-to-end vectors of chain segments between cross-links will be isotropically distributed. Assuming, for simplicity, that all proton pairs experience a unique residual dipolar splitting, $2\Delta_o = 2\nu_H P_2(\cos\vartheta)$, we may deduce that a single segment associated with a network chain end-to-end vector, **R**, oriented at angle θ to the magnetic field would present an apparent dipolar splitting of $2\Delta_o P_2(\cos\theta)$, while the static orientational average of all such isotropically distributed vectors (indicated by $\langle\ \rangle_s$) would result in a powder spectrum.

The second moment of a spectrum, $\Phi(\omega)$, is given by

$$\langle\Delta^2\rangle = \int_{-\infty}^{\infty} d\omega\ \Phi(\omega)\omega^2 \qquad (13)$$

For the dipolar interaction described, $\omega = \Delta_o P_2(\cos\theta)$, and, given an angular distribution $W(\cos\theta)$, we may write

$$\langle\Delta^2\rangle_s = \Delta_o^2 \int_{-1}^{1} d(\cos\theta)\ W(\cos\theta)[P_2(\cos\theta)]^2 \qquad (14)$$

The isotropic powder distribution, for which $W(\cos\theta)$ is unity, gives $\langle\Delta^2\rangle_s = (2/5)\Delta_o^2$, while a sample whose end-

to-end vectors {**R**} were all perfectly aligned with the magnetic field direction would give $\langle\Delta^2\rangle_s = 2\Delta_o^2$. By this simple argument, a factor of 5 range is available between the dipolar second moment of unstretched rubber and that of a sample in which all chains were aligned.

In fact, the simple reorientation argument just presented is somewhat naive. Any exact model that accounts for the influence of uniaxial stretching on the dipolar second moment for a polymer network must allow for several factors. First, it should take into account the distribution of end-to-end distances, R, and each of the corresponding segmental dipolar interactions, Δ_o, preexisting in the equilibrium state due to the statistics of the chains. Second, once the rubber is stretched, the chain end-to-end distances change, thus resulting in altered preaveraging motion and an altered magnitude of the residual dipolar interactions, Δ_o'. Finally, stretching along the direction of the magnetic field causes a realignment of the set of chain vectors {**R**} toward this direction and hence a change in the orientational distribution, $W(\cos\theta)$. Using such a simple model, Brereton[12] has calculated the spectral line shape, $\Phi(\omega,\lambda)$ resulting from an affine uniaxial stretching of Gaussian chains by a ratio $\lambda = L/L_0$, where L_0 and L are the lengths of the network along the stretching axis before and after extension. In the Brereton formulation, the residual dipolar interaction for a chain segment associated with an end-to-end vector **R** = (X,Y,Z) is given by

$$\Delta_o = \frac{\nu_H}{N}\left(\frac{2Z^2 - X^2 - Y^2}{Nb^2}\right) \tag{15}$$

where ν_H is the interaction strength in the absence of motional averaging and N is the number Kuhn statistical units, of size b, between cross-links. The resulting spectrum is given in terms of the parameter $\Omega = N\omega/\nu_H$ by[12]

$$\Phi(\omega,\lambda) = \Phi(0,1)[3/(2\lambda + \lambda^{-2})]^{1/2}\exp(-3\Omega\lambda/2)\{1 + \exp(3\Omega\lambda)\mathrm{erfc}([3\Omega(2\lambda + \lambda^{-2})/2]^{1/2}) \tag{16}$$

However, this expression is not consistent with the requirement of a constant area under the spectrum on deformation. Closer inspection of the derivation suggests that the correct result is[13]

$$\Phi(\omega,\lambda) = \Phi(0,1)[3/(2\lambda + \lambda^{-2})]^{1/2}\{\exp(-3\Omega\lambda) + \exp(3\Omega\lambda)\mathrm{erfc}([3\Omega(2\lambda + \lambda^{-2})/2]^{1/2}) \tag{17}$$

It may be shown[13] that eq 17 yields a second moment, which varies approximately as $\lambda^5/(2\lambda + \lambda^2) \approx \lambda^4$.

(ii) Unstretched Natural Rubber. We begin by considering dipolar interactions in undeformed natural rubber. Figure 3 (●) shows the results obtained for $\beta(2\tau,\tau)$ using the unstretched sample ($\lambda = 1$), where the time delay τ is varied from 0.1 to 4 ms in 24 steps, the entire experiment lasting <20 min. The data show clearly the dipolar sine correlation rising and then decaying in accordance with eqs 11 and 12. We have measured a value $T_2 = 6.5$ ms in this sample using the Ostroff−Waugh[14] sequence, $[90°_x-(\tau-90°_y-\tau-)_n]$, with $\tau = 0.05$ ms. Correcting the experimental $\beta(2\tau,\tau)$ data for this intrinsic relaxation, we can, according to eq 12, plot $\ln[\beta(2\tau,\tau)/(\tau^2\exp\{-2\tau/T_2\})]$ *vs* τ as shown in Figure 4 (○) to determine the correlation time governing the decay of the residual dipolar interactions, τ_Δ, from the slope and the magnitude of the interactions in terms of the second moment, $\langle\Delta^2\rangle$, from the intercept. Although for the $\lambda = 1$ network the semilog plot of the data exhibits a fairly linear dependence on τ over the entire range, we used the τ values for short times (●) to extract $\tau_\Delta = 0.52$ ms and $\langle\Delta^2\rangle = 1.2 \times 10^6$ rad^{2}s^{-2}, corresponding to the rising edge of the $\beta(2\tau,\tau)$ data, where the approximate expression eq 12 is valid. The solid line in Figure 3 is the theoretical result obtained from eq 12 (with the added factor $\exp\{-2\tau/T_2\}$ and the τ_Δ and $\langle\Delta^2\rangle$ values extracted from Figure 4); this result quantitatively describes the leading edge of the $\beta(2\tau,\tau)$ data and is in qualitative agreement with experiment across the entire range of τ.

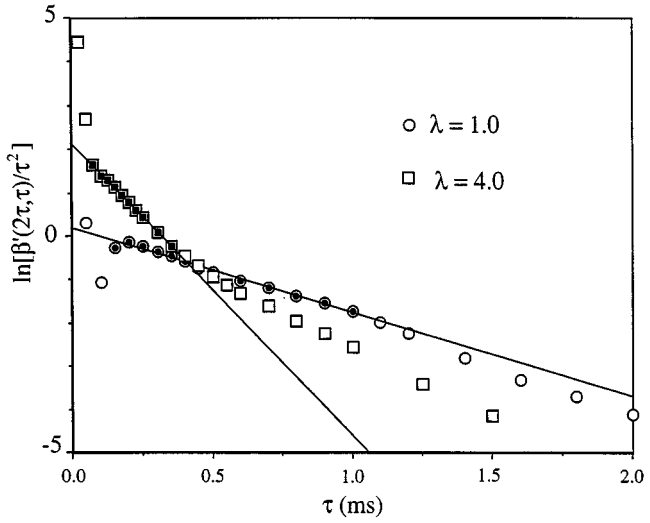

Figure 4. Typical plots of $\ln[\beta(2\tau,\tau)/(\tau^2\exp\{-2\tau/T_2\})]$ *vs* τ for a natural rubber network. $T_2 = 6.5$ ms and is independent of the deformation ratio λ. The initial points (filled symbols) were used in a least-squares fit to derive the second moment, $\langle\Delta^2\rangle$, from the intercept and τ_Δ from the slope (Tables 2 and 3).

(iii) Stretched Natural Rubber. In our initial investigation of uniaxial stretching in the rubber network, we have observed the effect of sample orientation on the β function at fixed extension ratios, $\lambda \approx 5$ and $\lambda \approx 2$. We were able to measure the angular dependence of $\beta(2\tau,\tau)$ using the Teflon goniometer shown in Figure 5. A glass capillary containing the approximately[15] uniaxially deformed network was inserted into the Teflon goniometer disk which was then oriented so that the extension axis subtended angles of $\theta_o = 0°$, 55°, and 90° with respect to the magnetic field. At these angles, the squared Legendre polynomial $[P_2(\cos\theta_o)]^2$ takes values of 1, 0, and $^1/_4$, respectively. The resulting experimental $\beta(2\tau,\tau)$ functions are shown in Figure 6, where it is immediately apparent that, for fixed orientation, a large increase in the value of $\langle\Delta^2\rangle$ has occurred on stretching—the leading edge of $\beta(2\tau,\tau)$ increases its slope and shifts to shorter times on deforming the network. The β function exhibits an orientation dependence that is more pronounced the larger the deformation; contrast the $\lambda \approx 5$ network observations (Figure 6B) with those of the $\lambda \approx 2$ network (Figure 6A). At each of the sample orientations θ_o, the corresponding values of τ_Δ and $\langle\Delta^2\rangle$ were extracted from semilog plots of the type shown in Figure 4. Table 2 shows that, on extension to $\lambda \approx 5$, the observed second moment increases by more than an order of magnitude. This finding is in contradiction with the simple argument presented above using eq 14 for $\langle\Delta^2\rangle_s$; we expect at most a factor of 5 increase for perfectly aligned chains with $\theta_o = 0°$. This contradiction emphasizes the necessity for addressing the changes that must occur in the

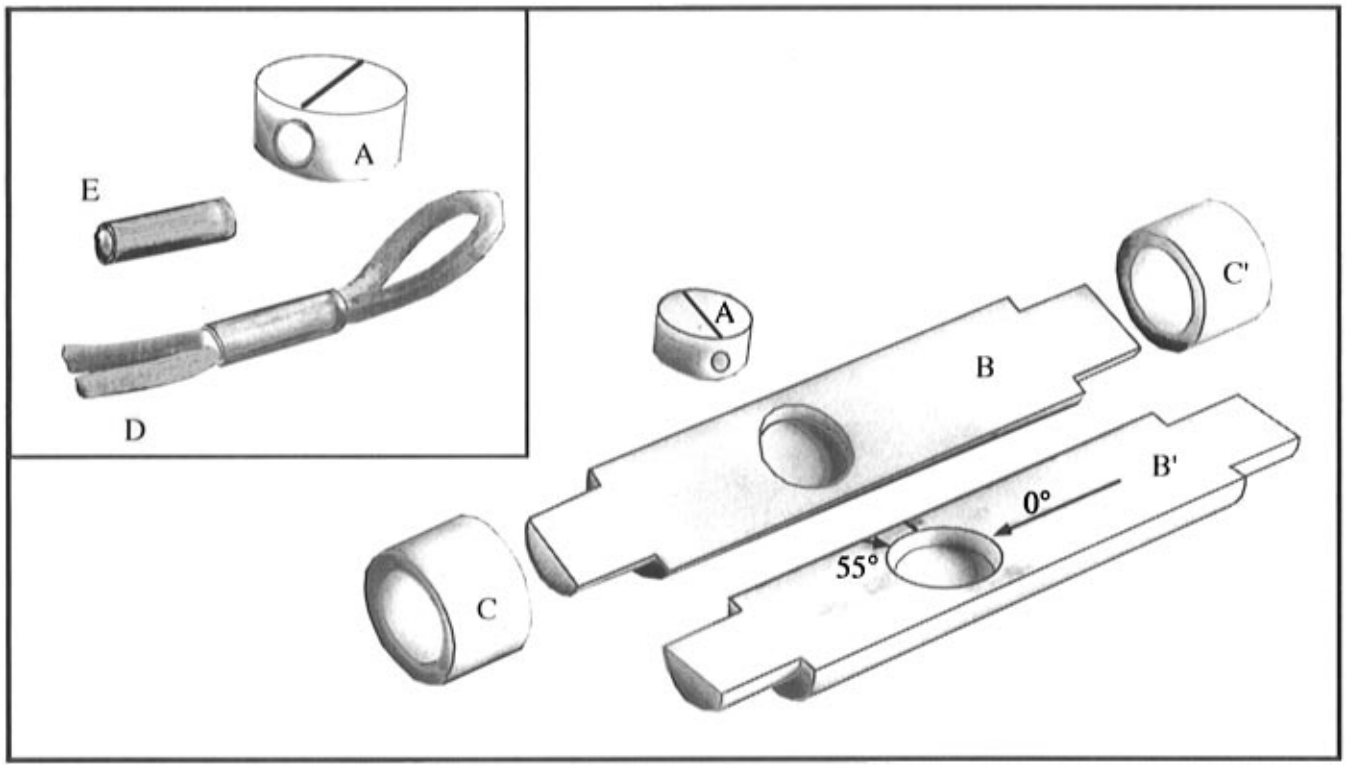

Figure 5. Teflon goniometer disk (A) and cylindrical Teflon casings (B,B′; 15 mm o.d.) with end-rings (C,C′). The device is used to orient the symmetry axis of uniaxially deformed rubber (D) held in the glass capillary insert (E) at specific angles relative to the spectrometer magnetic field ($\theta_o = 0°$, 90°, and 55°). The NMR experiments are performed with the goniometer/casing in a 15 mm diameter resonator.

Table 2. Angular Dependence of the Residual Second Moment, $\langle\Delta^2\rangle$, and Its Correlation Time, τ_Δ, of the Undeformed Natural Rubber Network ($\lambda = 1$) and at Two Extension Ratios, $\lambda \approx 2$ and $\lambda \approx 5$

λ	θ_o	$\langle\Delta^2\rangle$ (rad s^{-1})^2	τ_Δ (ms)
1		1.2×10^6	0.52
≈2	0°	5.5×10^6	0.18
	55°	4.2×10^6	0.20
	90°	3.9×10^6	0.22
≈5	0°	17.1×10^6	0.12
	55°	11.1×10^7	0.14
	90°	11.8×10^7	0.14

residual segmental dipolar interactions ($\Delta_o \rightarrow \Delta_o'$) when the chain vectors are (affinely) deformed. Additionally, the residual second moments found for the $\theta_o = 55°$ and 90° orientations are similar at both extensions ($\langle\Delta^2\rangle_{90°}/\langle\Delta^2\rangle_{55°} \approx 1$), while the ratio of the moments, $\langle\Delta^2\rangle_{0°}/\langle\Delta^2\rangle_{55°}$, changes modestly from 1.3 to 1.54 as λ is increased from 2 to 5.

These observations can be understood if one takes account of the static distribution of end-to-end vector orientations for chains between cross-links (or entanglements). The calculated 1, 0, and $^1/_4$ values for $[P_2(\cos\theta_o)]^2$ alluded to before for the three orientations $\theta_o = 0°$, 55°, and 90° correspond to the second moment scaling factors for chains that are perfectly aligned. As shown in Figure 7A, however, a small angular spread σ in the distribution in chain directors (modeled with a Gaussian distribution, $W(\cos\theta)$, about θ_o with variance σ^2) has the effect of compressing the calculated orientational dependence of the relative second moments $\langle\Delta^2\rangle_{\theta o}/\langle\Delta_o^2\rangle$, where the subscript characterizes the orientation of the static distribution. Forming the ratios from the calculated relative second moments in Figure 7A circumvents the uncertainties in the magnitude of Δ_o on extension and gives direct access to the calculated σ dependence of, for example, $\langle\Delta^2\rangle_{\theta o}/\langle\Delta^2\rangle_{55°}$. For mea-

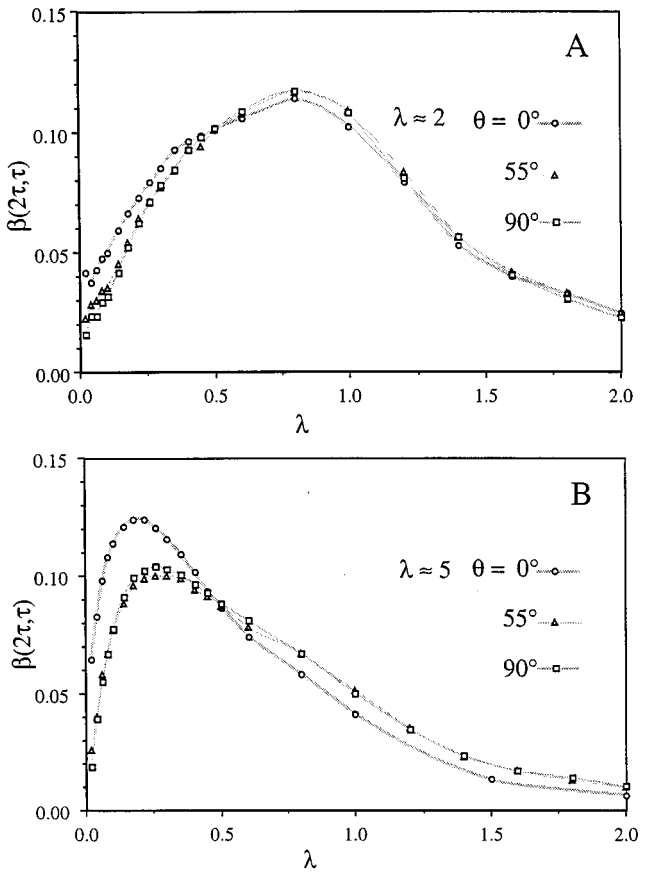

Figure 6. Orientation dependence of $\beta(2\tau,\tau)$ obtained from uniaxially deformed natural rubber samples. In both panels A ($\lambda \approx 2$) and B ($\lambda \approx 5$) the extension axis has been oriented with respect to the magnetic field at $\theta_o = 0°$ (○), 90° (□), and 55° (△). The gray interpolation lines are merely a guide to the eye.

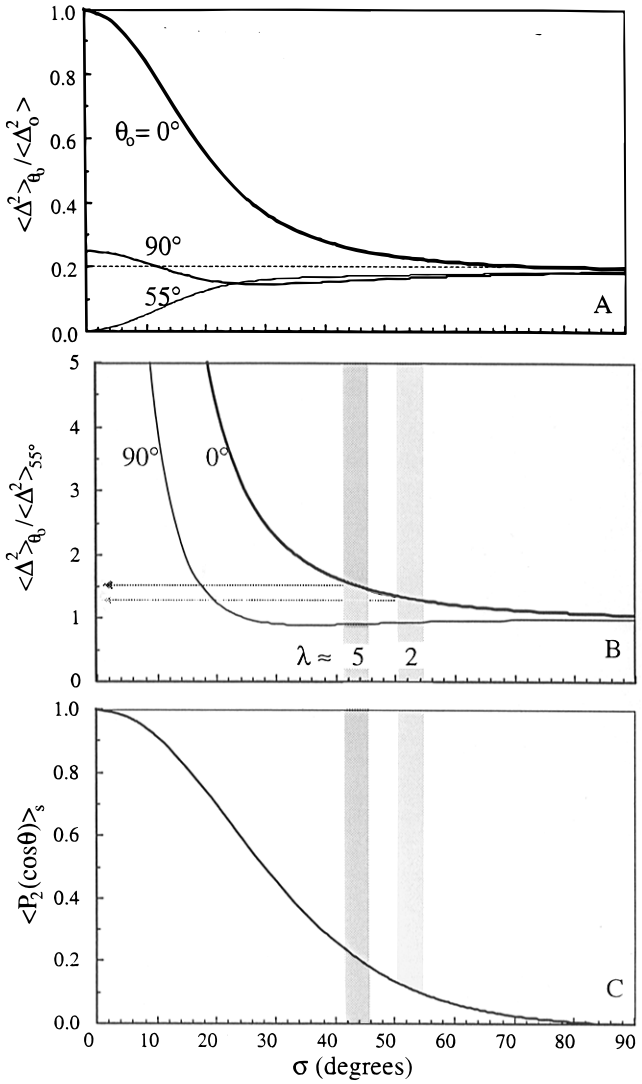

Figure 7. Calculated relative second moments (A), second moment ratios (B), and chain degree of order (C) for a static distribution of end-to-end vectors with a Gaussian spread of angles with variance σ^2 about the mean orientation θ_o relative to the magnetic field. In panel A, the static average of the second moment taken over the Gaussian spread is shown as a ratio to the value $\langle\Delta_o^2\rangle$. Results are shown for mean orientations of $\theta_o = 0°$, 90°, and 55°. The shaded bars correspond to the standard deviation (σ) of the angular distribution that fits the experimentally measured ratios $\langle\Delta^2\rangle_{\theta_0}/\langle\Delta^2\rangle_{55°}$ for $\theta = 0°$ and $\theta = 90°$.

surement at a given extension λ, a simultaneous fit of the experimental ratios $\langle\Delta^2\rangle_{90°}/\langle\Delta^2\rangle_{55°}$ and $\langle\Delta^2\rangle_{0°}/\langle\Delta^2\rangle_{55°}$ to calculated ratios (ordinate of Figure 7B) delineates a self-consistent range for the angular spread σ (shaded bars spanning the range on the abcissa of Figure 7). In turn, the σ range gives the corresponding magnitude of the degree of chain vector alignment—the intersection of shaded bar specifying the angular spread and the calculated static average $\langle P_2(\cos\theta)\rangle_s = \int \mathrm{d}\cos\theta P_2(\cos\theta)W(\cos\theta)$. Via this process, we derive $\langle P_2(\cos\theta)\rangle_s$ values of 0.1 and 0.2 corresponding to the network extensions $\lambda \approx 2$ and $\lambda \approx 5$, repectively (Figure 7C).

In our second set of experiments, we have carried out a series of measurements of the residual dipolar interactions in a rubber sample at fixed orientation ($\theta_o = 90°$) but stretched over a range of extension ratios up to $\lambda = 4$. The experiments were performed using a specially constructed jig similar to that diagrammed in Figure 3 of ref 16. The jig was used to controllably extend a

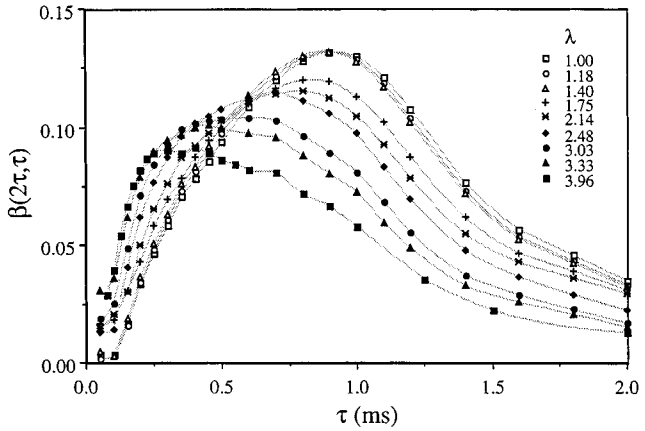

Figure 8. Family of $\beta(2\tau,\tau)$ functions obtained from the uniaxially extended sample of natural rubber in a transverse orientation ($\theta = 90°$). The grey lines are simply data interpolations provided to guide the eye.

Table 3. Angular Dependence of the Residual Second Moment, $\langle\Delta^2\rangle$, and the Apparent Correlation Time, τ_Δ, Governing the Loss of Dipolar Correlations in the Natural Rubber Network with Extension Ratio λ

λ	$\langle\Delta^2\rangle$ (rad s^{-1})^2 [a]	τ_Δ (ms)[a]
1.00	1.2×10^6	0.52
1.05	1.3×10^6	0.46
1.18	1.4×10^6	0.45
1.40	1.5×10^6	0.43
1.53	1.6×10^6	0.39
1.75	2.1×10^6	0.32
2.14	2.7×10^6	0.29
2.48	3.5×10^6	0.25
3.03	4.5×10^6	0.22
3.33	6.8×10^6	0.18
3.96	8.3×10^6	0.15

[a] Uncertainties in $\langle\Delta^2\rangle$ and τ_Δ are $\leq$ 10%.

rubber sample running through a solenoidal rf coil oriented normal to the magnetic field. Figure 8 shows the family of $\beta(2\tau,\tau)$ functions where there is an indication of a qualitative change in the profile of the function as the extension ratio exceeds $\lambda \approx 2$. The measured value of T_2 was essentially independent of extension. Hence, the apparent shift in the leading edge of the β function to shorter time with increasing λ can be analyzed as before with $\ln[\beta(2\tau,\tau)/(\tau^2\exp\{-2\tau/T_2\})]$ *vs* τ plots (Figure 4). In contrast with the findings at $\lambda = 1$, the semilog plot at high extensions shows considerable curvature (□ in Figure 4 are for $\lambda = 4$). Consequently, the inital slope (derived from ■) is used to determine the τ_Δ and $\langle\Delta^2\rangle$ values given in Table 3. This analysis shows a monotonic increase in the values of $\langle\Delta^2\rangle$ on stretching.

The values of the correlation time τ_Δ appear to decrease with increasing λ from a maximum value of 0.5 ms in the undeformed network. The reliability of the τ_Δ values derived from the semilog plots appears to be robust. For example, the τ_Δ values are independent of the magnitude of the second moment, as the ~20−70% variation in $\langle\Delta^2\rangle$ with the mean deformation direction θ_o (Table 2) does not manifest itself in the extracted values of τ_Δ using our analysis procedures. However, it is not obvious what kinds of λ-dependent dynamical processes are responsible for the loss of (residual) dipolar correlation (see Discussion).

In Figure 9A, we show the λ dependence of the residual dipolar interactions in terms of the observed $\langle\Delta^2\rangle$ (●) and the independently measured tensile force (○). The apparent qualitative change in the λ depen-

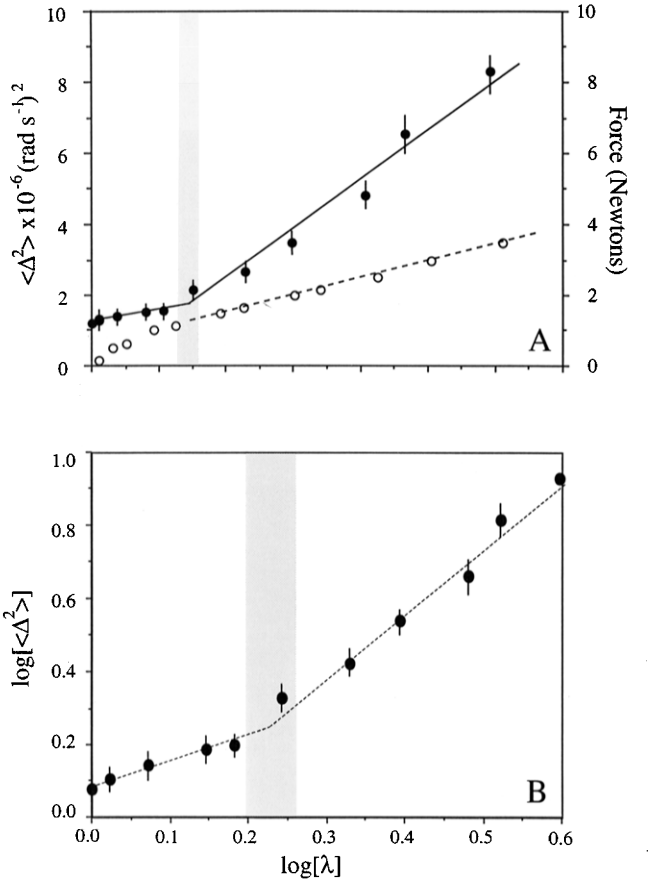

Figure 9. (A) Average residual second moments, $\langle\Delta^2\rangle$ (●), and the force (○) *vs* the extension ratio λ. The lines indicate that the qualitative trends in the data differ on either side of the shaded bar ($\lambda \approx 1.75$). (B) Log−log plot of the residual second moment *vs* the extension ratio. A change in scaling behavior is observed at the same extension ratio as the observed transition in elastic modulus.

dence of $\langle\Delta^2\rangle$ with network extensions above $\lambda \approx 1.75$ seems to be correlated with the initial deviation of the measured tensile force (or nominal stress of the initially ~1 mm^2 rubber network) *vs* λ curve from the classical statistical theory[17] of rubber elasticity (see Figure 5.4 in ref 18). Additionally, we observe from Figure 9B that the λ dependence of the value of $\langle\Delta^2\rangle$ is very much weaker than λ^4 predicted by the Gaussian model network calculation described above. Last, the break in the log−log plot shows that there does not appear to be a single scaling relation across the range of extensions we have explored.

Discussion

The small but finite residual dipolar interaction in natural rubber networks studied here may be viewed as if it were comprised of a rescaled static interaction—the preaveraged intrasegment dipolar interaction that is associated with each segment's respective network chain. Concomitantly, the rescaled interaction directions are transformed from the local interaction directions, the set of interproton vectors {**r**}, to {**R**}, the set of chain end-to-end vectors spanning the constellation of cross-links and entanglements in the network. We have demonstrated that changing the orientational distribution of {**R**} by uniaxial extension can perturb the magnitude of the residual dipolar interactions. Further, the observed changes in the magnitude of the residual second moment $\langle\Delta^2\rangle$ (>5 for extensions spanning $\lambda = 1-4$) implies that, in addition to changing the distribution of static **R** vectors, there is a change in the efficacy of the intrachain preaveraging, i.e., an accompanying change in the definition of the rescaled interaction $\Delta_o = \nu_H \overline{P_2(\cos\vartheta)}$ itself on stretching the network.

Using the $\lambda \approx 5$ results (Table 2) in conjunction with a Gaussian form for $W(\cos\theta)$ (where $\sigma \approx 45°$ is derived from fitting the ratios in Figure 7B), we would anticipate a 50% increase in $\langle\Delta^2\rangle$ (Figure 7A) from the associated orientational redistribution of the **R** vectors on stretching. But, in fact, we observe a 3-fold increase relative to the $\lambda = 1$ case, implying that $\overline{P_2(\cos\vartheta)}$ has also increased due to changing the length distribution of {**R**} by stretching. Thus, there exists clear evidence that the second moment increase does not arise from a change in the orientational distribution alone but also from a change in the preaveraged, intrasegment dipolar interaction as well.

Rapid fluctuations of **R** about its mean orientation—diffusive motions of the cross-link (entanglement) junctions—are subsumed into the preaverage of the dipolar interactions when the correlation time of such motions is sufficiently short (e.g., less than $\langle\Delta^2\rangle^{-1/2} \approx 10^{-3}-10^{-4}$ s for the rubber network considered herein). This contribution to the preaverage makes NMR residual dipolar and quadrupolar interations useful for characterizing networks since the magnitude of the incompletely averaged interactions and, particularly, their contribution to transverse relaxation—dipolar (quadrupolar) dephasing of the transverse magnitization—depend on the mean chain length between junctions, the fraction of pendant chains, etc.[19−21]

Random reorientations of **R** on a longer time scale would cause fluctuations in the (residual) dipolar interaction and ultimately lead to the decay of the phase angle correlation $\langle\sin\phi(0,\tau)\sin\phi(\tau,t)\rangle$, as expressed by eq 11 and implied by the experimental β function. However, it is difficult to propose plausible slow motional processes in the rubber that could lead to significant changes in the mean direction of **R** while simultaneously respecting the topology of the network. This perspective is reinforced by the recent measurements of Sotta and Deloche,[22] who infer that the residual quadrupolar interaction in deuterium-labeled polydimethylsiloxane networks is effectively static on a 10^{-1} s time scale. They show that the dynamics associated with the decay of the residual quadrupolar interaction are governed by the quadrupolar relaxation time, $T_{1Q} \approx 0.2$ s. This is accomplished by using the Jeener−Broekaert pulse sequence,[23] [90°$_x$−τ−45°$_y$−τ−45°$_y$], which refocuses only effectively static quadrupolar (dipolar) interactions. Application of the Jeener−Brockaert sequence to the natural rubber sample gives the corresponding dipolar relaxation time, T_{1D}. We find $T_{1D} = 30$ ms in the $\lambda = 1$ polyisoprene network, suggesting the residual dipolar interactions are static on the approximately 2 orders of magnitude smaller time scale, τ_Δ, governing the decay of the β function.

In attempting to interpret τ_Δ, it is important to reemphasize that eq 12 provides only an approximate representation of the "dipolar phase" sine correlation given in eq 11. Hence, the apparent value of τ_Δ will be strongly influenced by the assumptions inherent in the simple exponential correlation model and our use of the small phase angle approximation. A more detailed discussion of the time dependence of the sine correlation without the need for these assumptions will follow.[11] However, even within the simple theoretical framework

of the present discussion, it is clear that there exist additional mechanisms for the apparent decay associated with the rate τ_Δ^{-1}.

One candidate mechanism for this premature loss of dipolar correlation might be incomplete refocusing of higher order contributions to the dipolar echo. Consider the Bloch decay, as manifested in the signal acquired using the [90°$_x$−τ−180°$_y$] sequence, where no refocusing of dipolar dephasing occurs. This decay may be represented by the standard moment expansion,[24] $\exp[-(\tau^2/2!)M_2 + (\tau^4/4!)M_4 - ...)$, where M_n is the nth moment of the line shape, $\int_0^\infty d\omega\ \Phi(\omega)\omega^n$. As pointed out by Powles and Strange,[25] the solid echo pulse sequence refocuses the Bloch decay only partially. In particular, there remains from the fourth moment a residual component, $\tau^4 M_{4x}$, where M_{4x} involves interactions between more than two spins. Powles and Strange have shown, in the case of a rigid lattice, that $M_{4x} \approx (1/4)M_4 = (1/2)M_2^2$. By analogy, we would suggest that similar higher order multispin interactions (of order $\langle\Delta^2\rangle^2$), could lead to a diminution of the β function before it decays by intrinsic T_2 processes. Our observation that the decay rate τ_Δ^{-1} increases as M_2 increases is consistent with this viewpoint. However, given the "super-Lorentzian" character of the NMR line shape in rubber, we would expect that the ratio M_4/M_2^2 will be considerably higher than the value expected for a rigid lattice, where the line shape more closely approximates an ideal Gaussian form. Indeed, we find that our apparent τ_Δ values suggest $M_{4x} \approx 10M_2^2$ if the Powles and Strange mechanism is to be invoked.

Multispin interactions would complicate an underlying assumption of this study, namely, that the dipolar interactions are derived from isolated, pairwise interactions between the protons of polyisoprene. However, there is experimental evidence for the validity of a dominant two-spin approximation of the partially averaged dipolar interactions in polymer networks.[19,20] Using this approximation, we can get a sense of the efficacy of the fast preaveraging processes in the relaxed rubber by comparing the measured magnitudes of $\langle\Delta^2\rangle$ (Table 3) with the calculated static value of the second moment for rubber. To estimate the latter, it is necessary to make some idealizations of the polyisoprene molecular structure, $-[-CH_2CH{=}CCH_3CH_2-]_n$. If we assume that the proton pairs in the methylene groups of the isoprene units dominate the intramolecular residual dipolar interaction, we can calculate its static second moment,[24] $(9/20)\gamma^4\hbar^2 r^{-6} = 8.1 \times 10^9$ [rad s^{-1}]^2, where we have set $r = 0.178$ nm, the distance between a pair of geminal methylene protons. This value can be compared with the experimentally measured[26] rigid lattice second moment of solid polyisoprene below its glass transition, 12.9×10^9 [rad s^{-1}]^2, a number that includes both inter and intramolecular contributions. The static second moment is reduced by liquid-like local segmental mobility in the network, and we find that this fast reorientational motion of r results in a residual second moment, $\langle\Delta^2\rangle = 1.2 \times 10^6$ [rad s^{-1}]^2 ($\lambda = 1$). Hence, the ratio of the root-mean-square observed residual second moment, $\langle\Delta^2\rangle^{-1/2} = \nu_H\overline{P_2(\cos\vartheta)}$, to the rms calculated value, $[(9/20)\gamma^4\hbar^2 r^{-6}]^{-1/2}$, implies that the preaveraged residual dipolar interaction is roughly 1% of the static interaction, ν_H, i.e., the residual orientational order of the interproton axis r averaged over the fast segmental motions changes is $\overline{P_2(\cos\vartheta)} \approx 0.01$ in the relaxed network ($\lambda = 1$).

Summary

We have demonstrated here that it is possible to measure quite small proton dipolar interactions by the use of a pulse sequence that directly generates the superposition [$S_1 - S_2 - S_3$], where S_1, S_2, and S_3 are the respective signals arising from (90°$_x$−τ−90°$_y$), (90°$_x$−τ−90°$_x$), and (90°$_x$−τ−180°$_y$) spin echo experiments. The resulting echo function, which we term $\beta(2\tau,\tau)$, is independent of dephasing effects arising from magnetic inhomogeneity or chemical shifts, effects that would normally mask the dipolar interactions in conventional NMR spectroscopy and that prove extremely troublesome in other dipolar echo experiments, such as the Γ experiment of Cohen Addad.

The ability to avoid Zeeman dephasing is the key factor that enables the β experiment to be applied effectively in the case of proton NMR. This method, therefore, has the potential to be applied to a wide class of polymers, without the need for isotopic labeling and without significant regard to chemical shift complexities in the proton NMR spectrum. The fact that β is unperturbed by magnetic inhomogeneity is especially useful, since it allows weak dipolar interactions to be evaluated independent of sample geometry, thus enabling such measurements to be performed where the sample has an irregular shape or where it is contained in a vessel of magnetically undesirable symmetry, such as a Couette cell or cone-and-plate device.

In the experiments reported here, we have been able to measure β for the polymer protons in a natural rubber sample in two sample configurations: (i) a stretched network in a specially built extension rig placed inside the NMR probe and (ii) an extended rubber sample placed in a goniometer, which permitted rotation of the strain axis with respect to the polarizing field of the surrounding superconducting magnet. These experiments on extended rubber have revealed a number of interesting results. First, we have shown that the second moment of the line shape associated with the proton dipolar interaction can be extracted from the β function time dependence using a simple extrapolation procedure, which in our analysis is based on a single-exponential model for the dipolar echo decay. This decay appears to be more rapid than would be expected from fluctuations in the residual dipolar interactions associated with chain end-to-end vector reorientation, a view that is supported by the appearance of Jeener−Broekaert echoes on a time scale orders of magnitude larger than the apparent correlation time, τ_Δ. We believe that the most likely explanation for this decay is to be found by considering a more exact evaluation of the sine correlation expression, although we note that another contributing factor may be the influence of higher order spin interactions in the Bloch decay.

It is clear from the experiments performed here that the changes in the dipolar second moment observed when the rubber network is stretched arise both from a change in the preaveraging process (i.e., $\overline{P_2(\cos\vartheta)}$) and from a change in the orientational distribution of chain end-to-end vectors, {**R**}. We are able to separate these effects by measuring the dependence of the dipolar second moment on the angle subtended between the strain axis and the magnetic field axis. This method yields an estimate of the static distribution of chain end-to-end vectors that is independent of chain stretching effects. We find here that the dependence of the dipolar second moment on the uniaxial extension ratio, λ, is somewhat weaker than that predicted by the simple

Gaussian chain extension model of Brereton but stronger than would be predicted on the basis of chain reorientation alone.

We believe that our method for extracting information about small proton dipolar interactions has many potential applications in studies of polymer systems whose chain conformations and dynamics are constrained by topology in model networks. In subsequent publications, we will show that the delicate, residual proton dipolar order and its associated fluctuations can also be used to gain access to the molar mass dependence of slow dynamical processes in quiescent and sheared entangled polymer melts.

Acknowledgment. E.T.S. acknowledges support from the National Science Foundation (DMR-9412701) and the John Simon Guggenheim Foundation and the hospitality of the Department of Physics at Massey University, while P.T.C. acknowledges support from the New Zealand Foundation for Research, Science and Technology. We are grateful to Dr. Craig Eccles for help and advice concerning data processing and, in particular, for the use of his multidimensional data analysis program, PROSPA.

References and Notes

(1) Cohen Addad, J.-P. *J. Chem. Phys.* **1974**, *60*, 2440.
(2) Cohen Addad, J.-P. *Prog. NMR Spectrosc.* **1993**, *25*, 1 and references therein.
(3) Deloche, B.; Samulski, E. T. *Macromolecules* **1981**, *14*, 575.
(4) Deloche, B.; Beltzung, M.; Herz, J. *J. Phys. Lett.* **1982**, *43*, L763.
(5) Sotta, P.; Deloche, B. *Macromolecules* **1990**, *23*, 1999 and references therein.
(6) Samulski, E. T. *Polymer* **1985**, *26*, 177. Nakatani, A. I.; Poliks, M. D.; Samulski, E. T. *Macromolecules* **1990**, *23*, 2686.
(7) Cohen Addad, J.-P. *J. Chem. Phys.* **1975**, *63*, 4880 and references therein.
(8) Collignon, J.; Sillescu, H.; Spiess, H. W. *Colloid Polym. Sci.* **1981**, *259*, 220.
(9) Ernst, R. R.; Bodenhausen, G.; Wokaun, A. *Principles of Nuclear Magnetic Resonance in One and Two Dimension*; Oxford University Press: Oxford, U.K., 1987.
(10) Callaghan, P. T. *Polymer* **1988**, *29*, 1951.
(11) Ball, R. C.; Callaghan, P. T.; Samulski, E. T. To be published.
(12) Brereton, M. G. *Macromolecules* **1993**, *26*, 1152.
(13) Warner, M.; Callaghan, P. T.; Samulski, E. T. To be published.
(14) Ostroff, E. D.; Waugh, J. S. *Phys. Rev. Lett.* **1966**, *16*, 1097.
(15) The highly deformed rubber network is drawn through the tight-fitting capillary and then allowed to relax, contracting slightly and expanding against the capillary walls. The (isotropic) ends of the rubber can then be cut off without significant further contraction, thereby maintaining an approximately uniaxial strained network in the gonometer (see Figure 5).
(16) Dardin, A.; Boeffel, C.; Spiess, H.-W.; Stadler, R.; Samulski, E. T. In *Flow-Induced Structure in Polymers*; Nakatani, A. I.; Dadmun, M. D., Eds.; ACS Symposium Series 597; American Chemical Society: Washington, DC, 1995; p 190.
(17) Kuhn, W. *Kolloid-Z.* **1936**, *101*, 248.
(18) Treloar, L. R. G. *The Physics of Rubber Elasticity*, 3rd ed.; Oxford University Press: London, 1975.
(19) Simon, G.; Baumann, K.; Gronski, W. *Macrolmolecules* **1992**, *25*, 3624.
(20) Sotta, P.; Fulber, C.; Demco, D. E.; Blumich, B.; Spiess, H. W. *Macrolmolecules*, submitted.
(21) McLoughlin, K.; Szeto, C.; Duncan, T. M.; Cohen, C. *Macrolmolecules*, submitted.
(22) Sotta, P.; Deloche, B. *J. Chem. Phys.* **1994**, *100*, 4591.
(23) Jeener, J.; Broekaert, P. *Phys. Rev.* **1967**, *157*, 232.
(24) Abragam, A. *The Principles of Nuclear Magnetism*; Oxford University Press: Oxford, U.K., 1961.
(25) Powles, J. G.; Strange, J. H. *Proc. Phys. Soc.* **1963**, *82*, 6.
(26) Gutowsky, H. S.; Saika, A.; Takeda, M.; Woessner, D. E. *J. Chem. Phys.* **1957**, 534.

MA960784U